

## Experimental and analytical analysis of spot-welded cold form steel built up section under axial compression

Anitha Raneer Ramasamy Tamilarasa<sup>1</sup> , Srisanthi Vellalapalayam Gurusamy<sup>2</sup>

<sup>1</sup>Jai Shriram Engineering College, Department of Civil Engineering, Tiruppur, India.

<sup>2</sup>Coimbatore Institute of Technology, Department of Civil Engineering, Coimbatore, India.

e-mail: anitharaneer@gmail.com, srisanthivg@gmail.com

---

### ABSTRACT

The widespread adoption of Cold-Formed Steel (CFS) sections for constructing cost-effective housing and lightweight industrial structures is attributed to their ease of assembly and earthquake-resistant properties. Substantial research efforts have focused on enhancing the cost efficiency of structures by utilizing assembled CFS sections. The effectiveness of these BU-C sections relies on their ability to function in a composite manner, a function influenced by the type and arrangement of connections. The study encompasses both experimental and finite element analysis, involving 27 axial compression tests. These tests were conducted on specimens with varying cross-sections and thicknesses, each tested at different pitches. The experimental findings indicate a significant increase in axial compression load when number of pitch is increased. An ABAQUS-based Finite Element Model (FEM) was formulated and validated against the experimental data, demonstrating consistency in both axial compression load and buckling behavior. This authenticated FEM was subsequently employed for a parametric investigation, exploring the impact of pitch, spot welding thickness, and length on the axial compression capacity of BU-C. The observation was that an increase in pitch enhances the composite behavior of CFS BU-C, leading to a corresponding augmentation in compression capacity.

**Keywords:** Cold formed steel Sections; Built Up Channels; Spot Welding; Finite Element Model.

---

### 1. INTRODUCTION

The utilization of CFS has gained significant prominence within the field of structural engineering in recent years. This is attributed to their numerous advantageous properties such as rapid construction, space-saving attributes, and aesthetic appeal, among others. In parallel, there has been a notable rise in the use of BU-C, achieved by either combining two commercially available prefabricated channels in a back-to-back configuration or fabricating channels according to a specific design and then joining them. BU-C composed of cold-formed steel offer effective solutions for structures subjected to higher axial compression. The load-carrying capacity, as well as the torsional and flexural rigidity of built-up sections increases to a greater extent than the simple arithmetic sum of individual sections [1–3]. The load carrying capacity of CFS BU sections are influenced by slenderness ratio, interconnections by battens [4], stiffeners [5–7], provision of lipped channels [8, 9], cross sectional configuration [10–12], Further load carrying capacity of CFS BU sections improves when monolithic behavior is achieved for which provision of fasteners like screws, bolts, spot welding plays an important role [13–18].

Use of Abaqus, Finite Element Analysis software has become widespread due to its increased computational powers. Abaqus offers solution to sophisticated structural engineering problems. Once its results get validated it, can be used for wide parametric studies. Results of numerical studies are generally more than design standards [19, 20]. Effective width formula and Direct Strength Method (DSM) [21–23]. Finite Element Model (FEM) created by researchers to analyze the structural behavior of cold-formed high-strength stainless steel columns with square and rectangular hollow sections under fixed end boundary conditions and validated using experimental results for various column lengths revealed that the design standards were generally conservative for cold-formed high-strength stainless steel square and rectangular hollow section columns, but they proved to be un-conservative for some of the short columns [24–26].

### 1.1. Research objectives

Guidelines for the design of Cold-Formed Steel (CFS) built-up members joined through spot welding are scarce. Limited research has been dedicated to CFS Built-Up Channels (BU-C) with spot welding connections. Additionally, existing design standards, such as those found in the AISI code, Euro code, and AS/NZS codes, [19, 20] do not encompass provisions for various parameters specific to CFS BU-C with spot welding connections. Current design specifications for CFS built-up members lack explicit design parameters that consider the influence of pitch on axial compression load capacity. The AISI design standard [19, 20], for instance, addresses this by adjusting the section slenderness through modifications to the global slenderness expressions as outlined below

$$\left(\frac{KL}{r}\right)_m = \sqrt{\left(\frac{KL}{r}\right)_0^2 + \left(\frac{a}{r_i}\right)^2} \quad (1)$$

Where  $KL/r$  = Slenderness ratio of entire section about governing axis of CFS BU-C

$a$  = Spacing between the intermediate self drilling fastener

$r$  = radius of gyration of the governing axis of the full cross section for CFS BU-C

$r_i$  = radius of gyration of the governing axis of the full cross section for individual section

$K$  = Effective length factor for concentrically loaded compression member

### 1.2. Research uniqueness

The current research encompasses both experimental and numerical investigations, which are focused on examining the composite behavior of CFS BU-C, identifying prevalent buckling modes, and understanding the failure modes in a series of 27 spot-welded CFS BU-C specimens.

The specimens utilized in this research exhibit a unique characteristic, as they entail the construction of built-up channels through spot welding of two separate lipped 'L' sections. Notably, one of these lips is inclined at an angle of 135 degrees, in contrast to the conventional 90-degree orientation observed in available market sections. The primary objective of the research is to gain a comprehensive understanding of effect of pitch, BU-C thickness, and length on the structural performance of BU-C when subjected to axial compressive loads. To facilitate the investigation, advanced shell finite element models have been developed with the ABAQUS software. These models have been rigorously validated using experimental test results. These validated models represent invaluable tools for future studies, potentially negating the necessity for additional physical testing

## 2. MATERIALS AND METHODS

### 2.1. Materials

AISI [19, 20] recommends that the steel utilized in cold forming should possess yield strength within the range of 172 to 482 MPa and an ultimate tensile strength within the range of 289 to 584 MPa. AISI specifies that the ratio of tensile strength to yield strength should fall within the range of 1.21 to 1.80. The minimum elongation percentage, according to AISI, should be in the range of 12 to 27 percent. The values of the modulus of elasticity, yield stress, and ultimate stress obtained through the tensile coupon test of the steel utilized in the experiment are presented in Table 1. It is evident from the table that the values of these various parameters align with the specifications outlined by AISI.

### 2.2. Material properties

The material characteristics of the CFS (Cold-Formed Steel) sections were determined through tensile coupon tests. These coupons were derived from break-pressed CFS sections, and their dimensions adhered to ASTM

**Table 1:** Mechanical properties of cold form steel sheets subjected to coupon tests.

| S NO | THICKNESS OF SHEET | E (Mpa)                | F <sub>y</sub> (Mpa) | F <sub>u</sub> (Mpa) | F <sub>u</sub> /F <sub>y</sub> |
|------|--------------------|------------------------|----------------------|----------------------|--------------------------------|
| 1.   | 0.80               | 2.05 × 10 <sup>5</sup> | 273                  | 360                  | 1.32                           |
| 2.   | 1.00               | 2.00 × 10 <sup>5</sup> | 285                  | 370                  | 1.30                           |
| 3.   | 1.20               | 2.10 × 10 <sup>5</sup> | 297                  | 390                  | 1.31                           |



Figure 1: Tensile coupon test of Specimen.

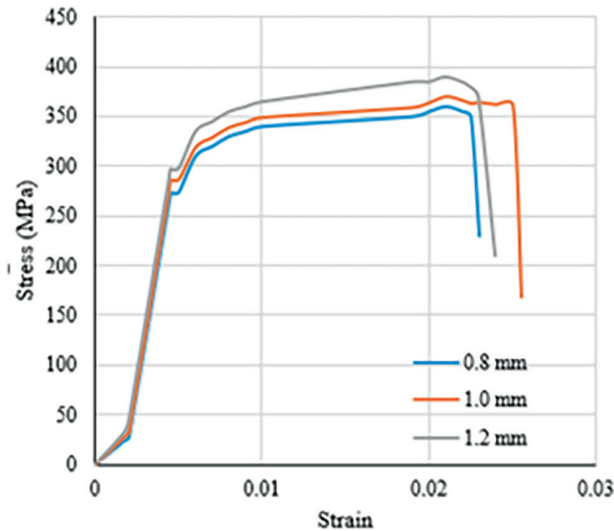


Figure 2: Stress strain curve.

(E8) standards [27], and as specified by HUANG and YOUNG [28]. The tests were conducted using a universal testing machine equipped with special grips designed to securely hold the coupons. Figure 1 shows coupon test of the specimen before and after failure. Figure 2 shows the stress strain curve of the material.

### 3. EXPERIMENTAL TESTING

#### 3.1. Test specimens

The test specimens of CFS BU-Care brake pressed from structural steel sheet to form the required open CFS profile, and then two of the open CFS profiles were connected at their web by spot welding to form CFS BU-C as shown in Figure 3. Dimensional details of CFS BU-C are also given in Figure 3.

Total of 27 specimens as shown in Figure 4 were fabricated. Specimens were made for a length of 1000 mm. Ends of specimen was milled for even finish and then welded to 10 mm thick mild steel plate on both ends to ensure full contact between specimen and end bearings.

Each Section has three different thicknesses of 0.8 mm, 1.0 mm and 1.2 mm. Each thickness intern has three different pitches of spot welding. Details of cross section profile were shown in Figure 3. The test specimens are categorized into three series according to their profile thickness. The specimens are labeled in such a way that the profile thickness and spot welding layout could be identified from the label. For example, the labels “BU-C0.8P2” and “BU-C1.2P10” define the specimens as follows:

The first three letters “BU-C” refers to built up-channels.

The fourth and fifth letters “0.8” refers to BU-C thickness in mm.

The six letter “P” refers to pitch.

The seventh letter onwards “2” and “10” refers to pitch of spot welding in numbers as given in Figure 3. To connect two individual CFS profiles spot welding was done 50 mm away from the mild steel end plates, after this weld, in the longitudinal direction three different layout of spot welding were used as shown in Figure 3. Spot welding was done as per AISI 2016 [19, 20] standards and also from inputs of UNGUREANU *et al.* [29] who has done experimental and numerical investigations on built-up CFS beams using resistance spot welding. The diameter of resistance spot welding was 4.00 mm.

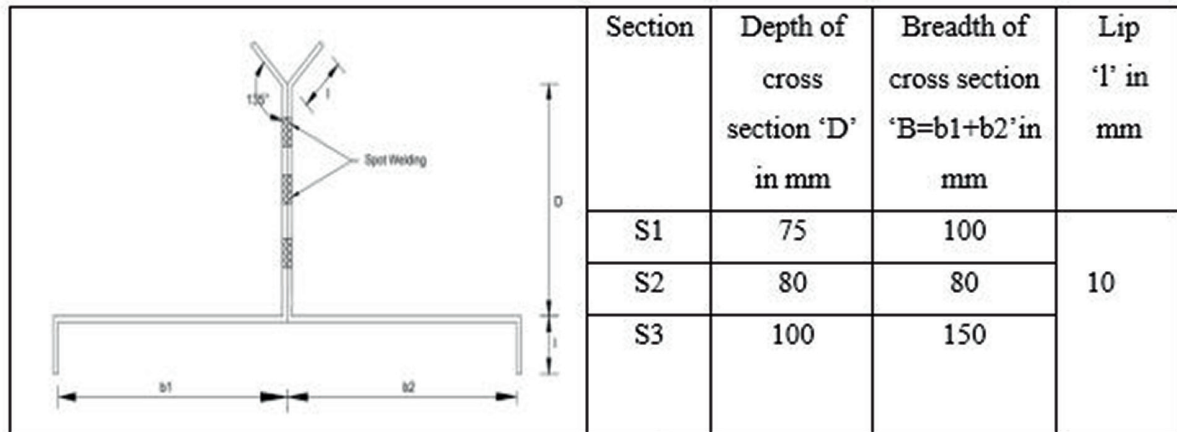


Figure 3: CFS BU-Columns with three rows of spot welding.



Figure 4: 27 numbers of CFS BU-C.

### 3.2. Setup of test

Loading setup on the load frame for CFS BU-C are shown in Figure 5. Compression testing machine with Data Acquisition system was used for testing of CFS BU-C. The adjustable top end support allowed fixing of CFS BU-C. Rigid Base plate was provided on both end of CFS BU-C by welding steel base plate to prevent major and minor axis rotation and to provide fixed end condition [30]. Centre of gravity of CFS BU-C is aligned with center of gravity of loading piston by vertical spirit level from all four sides of the specimen to be tested.

### 3.3. Axial shortening

In general, all 27 tested built-up columns showed elastic behaviour at initial stage of loading. Relation between compression resistance and axial shortening was noticed as linear for the first three fourth of the value and after that it was non linear till its failure. For S1BU-C, for three different values of pitch 2, 6, 10 and for thickness 0.8 mm, 1 mm and 1.2 mm the axial shortening graph obtained is shown in Figure 6. As expected, it was observed that axial compression is inversely proportional to number of pitches. The effect of pitch on axial compression is shown in Figure 6.

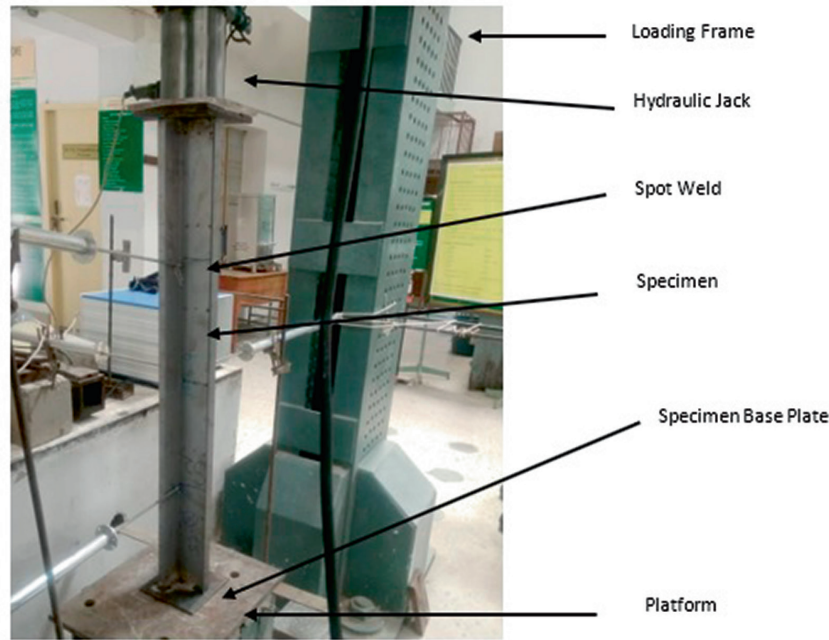


Figure 5: Test set-up.

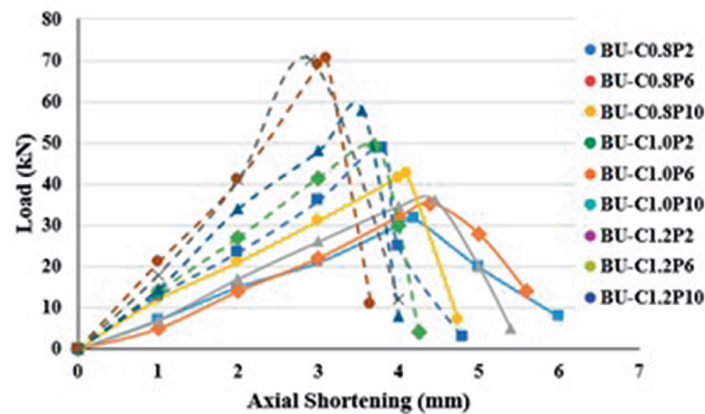


Figure 6: Axial Compression Load vs axial shortening of CFS BU-C for S2.

## 4. FINITE ELEMENT MODELING

### 4.1. General

The finite element (FE) software Abaqus/CAE version 2020 was used to create FE models of tested CFS, built-up sections as shown in Figure 7 to analytically predict the behavior of CFS BU-C sections and their compression capabilities. Guidelines given in the Abaqus user manual were followed while developing FE models. Details like perfect section geometry, end conditions and material properties were fed into the software. In the FE analysis, non-linear analyses were performed to obtain the ultimate loads and deformed shapes. At the end of the analyses, due to the complex geometric shape of built-up sections, modified Riks nonlinear solver was applied.

### 4.2. Element type

The S4R elements were used to model the elements of each built-up section. The utilized model was a fournode, quadrilateral stress/displacement shell element with reduced integration and a large strain formulation. The S4R element can be used for a very large area of applications including thinwalled structures like CFS members. Also, the S4R element is found to be computationally efficient. A mesh of 10 mm × 10 mm as shown in Figure 8 and 9 below were selected.

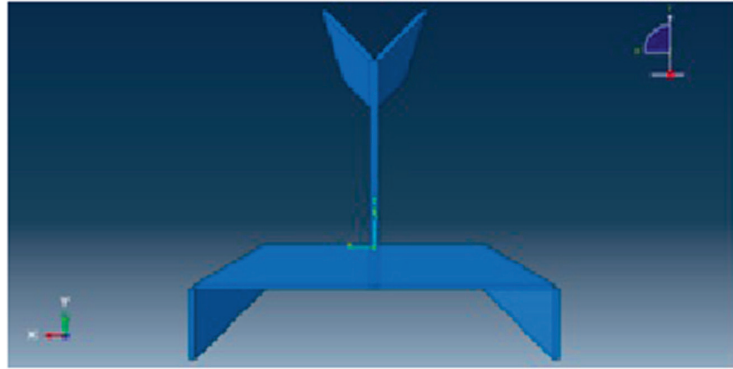


**Figure 7:** FE model of specimen.

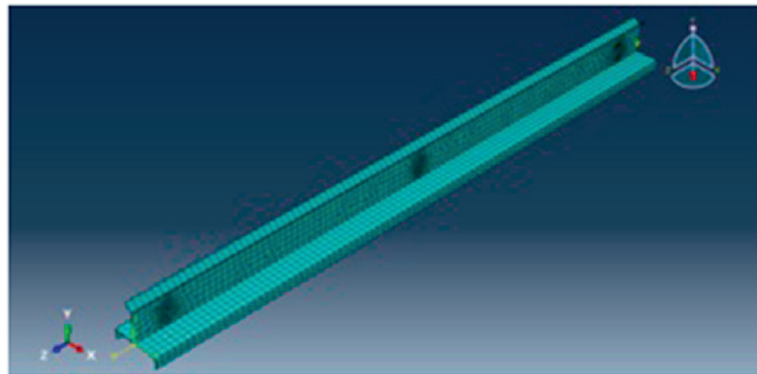


**Figure 8:** FE mesh of BC member-3D view.

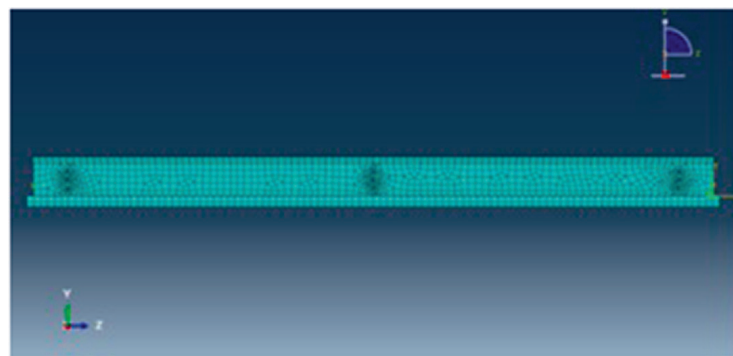


**Figure 9:** Side view showing FE mesh of BC member including spot welding.

#### **4.3. Material properties**

The material properties were derived from tensile coupon tests for 0.8 mm, 1.0 mm and 1.2 mm thick cold-formed steel. Values obtained from tensile coupon tests such as yield stress  $f_y$ , ultimate stress  $f_u$  and young's modulus  $E$  which are given in Table 1 above were used to develop the model.

#### **4.4. Boundary condition and loading method**

Consistent with the test setup, fixed end boundary conditions were applied in all Abaqus models of built-up sections used in this research. Displacements  $U_x$ ,  $U_y$  are restrained at top and bottom while displacement along  $z$  direction,  $U_z$ , is unrestrained at the bottom alone. Rotations in all three directions are restrained both at top and bottom.

#### **4.5. Interactions in the BC member**

The BC member used in research is a complex space since it is symmetrical along one axis only (singly symmetrical and not doubly symmetrical) as a result, the interactions between elements in each member are intricate.

To address this complexity, the Abaqus models of BC members utilized ‘general contact’ with ‘hard contact’ normal behavior. A friction coefficient of 0.19 was adopted to represent the interaction between individual members forming connections by spot welding for joining two individual members, Abaqus ‘point based’ fasteners as shown in Figure 9 were used. Of the three basic categories of connections in Abaqus, “translational basic connection” was selected, under this “Cartesian” type was selected.

## 5. RESULTS AND DISCUSSION

### 5.1. Experimental findings

Experiments were conducted on 27 CFS BU-C comprising of three different sections S1, S2, S3 and for three different thicknesses 0.8 mm, 1.0 mm, 1.2 mm along with three different pitch value 2, 6 and 10 as shown in Table 2. From the axial compressive load value obtained, it is inferred that there is an increase in axial load of CFS BU-C0.8 by 11.12%, 12.14% and 10.25% in S1, S2 and S3 respectively whose B/D ratio were 1.33, 1 and

**Table 2:** Table showing values of Nc Test, Nc FEA and failure mode.

| S NO | SECTION | SPECIMEN   | DEPTH<br>'D' IN<br>mm | BREATH<br>'B' IN<br>mm | NC,<br>TEST<br>(kN) | NC, FEA<br>(kN) | NC FEA/<br>NC TEST | FAILURE<br>MODE | B/D  |
|------|---------|------------|-----------------------|------------------------|---------------------|-----------------|--------------------|-----------------|------|
| 1.   | S1      | BU-C0.8P2  | 75                    | 50 + 50                | 36.025              | 35.3045         | 0.98               | FT              | 1.33 |
| 2.   | S1      | BU-C0.8P6  | 75                    | 50 + 50                | 40.031              | 45.23503        | 1.13               | FT              | 1.33 |
| 3.   | S1      | BU-C0.8P10 | 75                    | 50 + 50                | 41.18               | 43.6508         | 1.06               | FT              | 1.33 |
| 4.   | S1      | BU-C1.0P2  | 75                    | 50 + 50                | 48.793              | 45.37749        | 0.93               | FT              | 1.33 |
| 5.   | S1      | BU-C1.0P6  | 75                    | 50 + 50                | 53.784              | 58.08672        | 1.08               | FT              | 1.33 |
| 6.   | S1      | BU-C1.0P10 | 75                    | 50 + 50                | 56.253              | 54.56541        | 0.97               | FT              | 1.33 |
| 7.   | S1      | BU-C1.2P2  | 75                    | 50 + 50                | 61.098              | 69.04074        | 1.13               | F               | 1.33 |
| 8.   | S1      | BU-C1.2P6  | 75                    | 50 + 50                | 66.817              | 68.82151        | 1.03               | F               | 1.33 |
| 9.   | S1      | BU-C1.2P10 | 75                    | 50 + 50                | 70.947              | 71.65647        | 1.01               | FT              | 1.33 |
| 10.  | S2      | BU-C0.8P2  | 80                    | 40 + 40                | 34.465              | 33.7757         | 0.98               | FT              | 1.00 |
| 11.  | S2      | BU-C0.8P6  | 80                    | 40 + 40                | 38.649              | 39.42198        | 1.02               | FT              | 1.00 |
| 12.  | S2      | BU-C0.8P10 | 80                    | 40 + 40                | 39.727              | 41.71335        | 1.05               | FT              | 1.00 |
| 13.  | S2      | BU-C1.0P2  | 80                    | 40 + 40                | 46.01               | 46.9302         | 1.02               | FT              | 1.00 |
| 14.  | S2      | BU-C1.0P6  | 80                    | 40 + 40                | 51.185              | 53.2324         | 1.04               | FT              | 1.00 |
| 15.  | S2      | BU-C1.0P10 | 80                    | 40 + 40                | 52.667              | 56.35369        | 1.07               | FT              | 1.00 |
| 16.  | S2      | BU-C1.2P2  | 80                    | 40 + 40                | 58.336              | 68.25312        | 1.17               | FT              | 1.00 |
| 17.  | S2      | BU-C1.2P6  | 80                    | 40 + 40                | 64.508              | 67.7334         | 1.05               | FT              | 1.00 |
| 18.  | S2      | BU-C1.2P10 | 80                    | 40 + 40                | 66.299              | 71.60292        | 1.08               | FT              | 1.00 |
| 19.  | S3      | BU-C0.8P2  | 100                   | 75 + 75                | 46.213              | 46.67513        | 1.01               | F               | 1.50 |
| 20.  | S3      | BU-C0.8P6  | 100                   | 75 + 75                | 50.95               | 52.4785         | 1.03               | FT              | 1.50 |
| 21.  | S3      | BU-C0.8P10 | 100                   | 75 + 75                | 54.342              | 53.25516        | 0.98               | FT              | 1.50 |
| 22.  | S3      | BU-C1.0P2  | 100                   | 75 + 75                | 62.498              | 61.87302        | 0.99               | F               | 1.50 |
| 23.  | S3      | BU-C1.0P6  | 100                   | 75 + 75                | 68.354              | 73.13878        | 1.07               | FT              | 1.50 |
| 24.  | S3      | BU-C1.0P10 | 100                   | 75 + 75                | 73.872              | 80.52048        | 1.09               | FT              | 1.50 |
| 25.  | S3      | BU-C1.2P2  | 100                   | 75 + 75                | 77.328              | 88.15392        | 1.14               | F               | 1.50 |
| 26.  | S3      | BU-C1.2P6  | 100                   | 75 + 75                | 84.256              | 81.72832        | 0.97               | FT              | 1.50 |
| 27.  | S3      | BU-C1.2P10 | 100                   | 75 + 75                | 89.398              | 88.50402        | 0.99               | FT              | 1.50 |
|      |         |            |                       |                        |                     | Mean            | 1.03               |                 |      |
|      |         |            |                       |                        |                     | COV             | 0.06               |                 |      |

1.5, when pitch increase from 2 to 6. Similarly, the increase in axial compressive load of CFS BU-C noted to be 14.31%, 15.27% and 17.59% for S1,S2,S3 when pitch increases from 2 to 10.

From the failure behaviour of CFS BU-C, it is inferred that increase in the breadth of specimen affects the buckling nature of the CFS BU-C by preventing the section from undergoing major torsional buckling thus stiffening the column as shown in Figure 10 for S3 whose B/D ratio is 1.5. The failure mode of column mainly is due to lack of composite action of column in case of low pitch specimen as shown in Figure 10, S3BU-C0.8P2. The same section with higher pitch value of 6 and 10 shows torsional flexural bending mode with well connected composite action in failure as shown in Figure 10, S3BU-C0.8P6 and S3BU-C1.0P10. As the thickness of specimen for higher B/D increases, the lack of composite action is visible even in pitch 10 specimen as shown in Figure 10, S3BU-C1.2P10 which is similar to that of pitch 2 specimen S3BU-C1.2P2, but the difference is axial deformation of pitch 2 specimen is less compared to axial deformation due to pitch 10 specimen and axial load capacity of pitch 10 is 15.61% higher than the axial capacity of pitch 2 specimen. This implies that for higher thickness along with higher B/D ratio, number of spot weld in a row along with pitch should be increased and given more importance to increase the axial load capacity of CFS BU-C. For S1 and S2, whose B/D ratio value for built up section is 1 and 1.33 respectively, the failure of section is predominantly flexural torsional mode as shown in Figure 10 and composite action prevails for 2, 6 and 10 pitch for all three thickness as shown below except for S1 of thickness 1.2 and pitch 2.

### 5.2. Simulation results

The deformed shapes of CFS BU-C specimens observed during tests were shown in Figure 11 exhibit a remarkable similarity to those obtained from Finite Element (FE) analyses. However, the variation between the actual result and abacus was around 1%, as shown in Figure 12. This could be due to human errors during the fabrication of built-up sections. Nonetheless, the developed Finite Element (FE) models are deemed reliable for accurately predicting the compression capacity of built-up sections.



Figure 10: Deformed shapes of specimen after experiments.

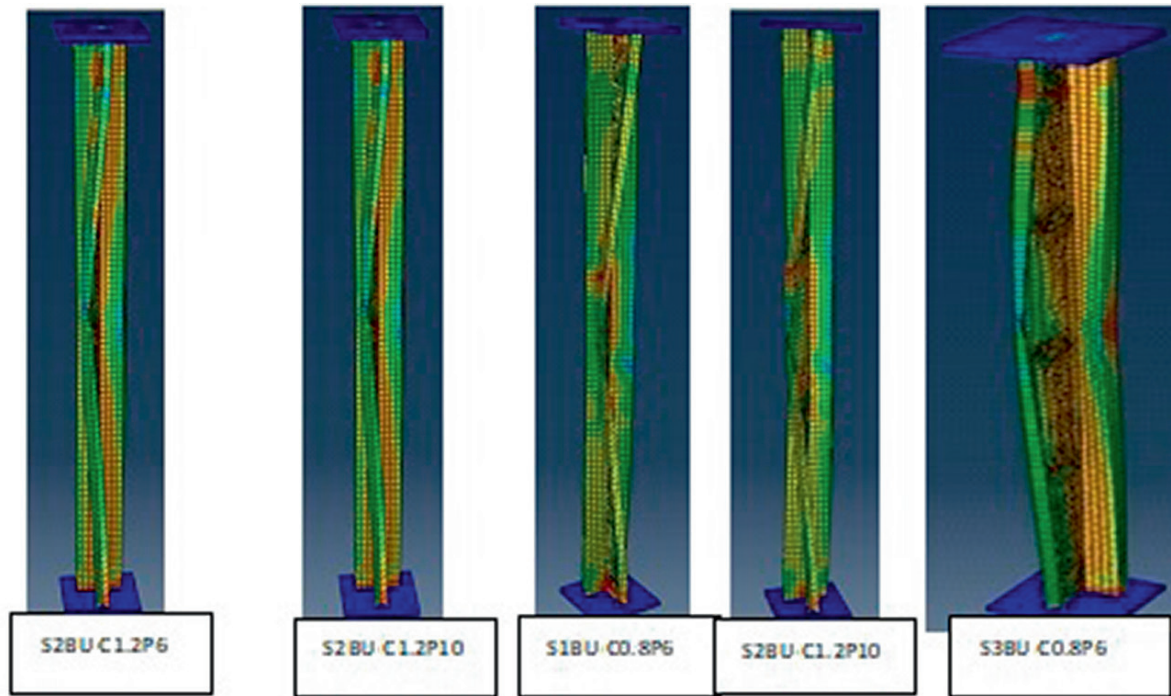


Figure 11: ABAQUS simulated deformed shapes of BU-C.

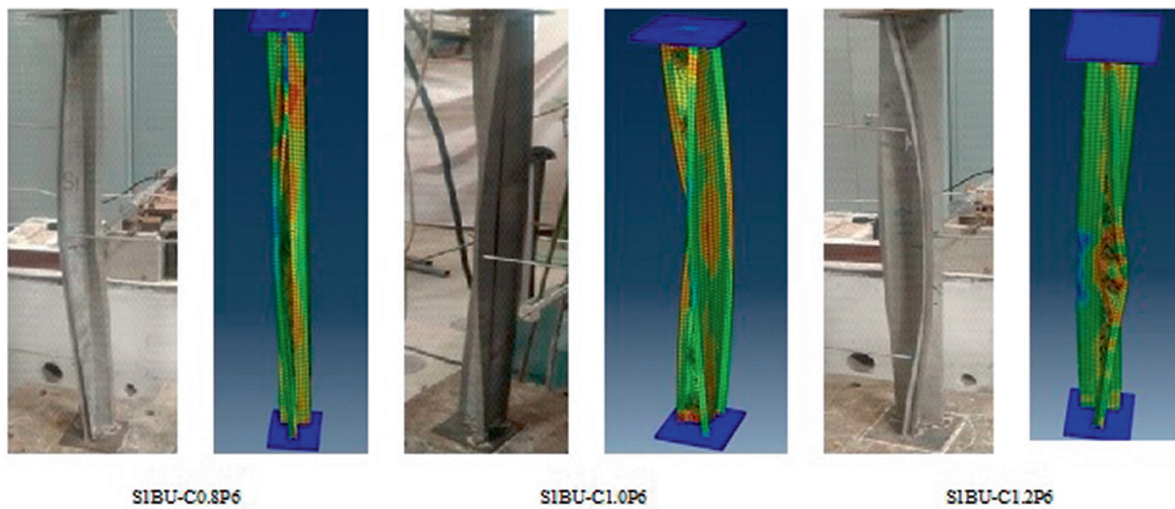


Figure 12: Comparison of test results with simulated results.

## 6. PARAMETRIC STUDIES

The FE models developed were confirmed with the experimental results and this confirmed FE models were further used for parametric studies on the effect of pitch, thickness of CFS sections and length on CFS BU-C columns.

### 6.1. Effect of pitch

It may be observed from the experimental values for 0.8 mm thick specimen, there is an increase in axial load capacity of CFS BU-C0.8 by 11.12 %, 12.14% and 10.32% when pitch raised from 2 to 6 and an increase of 14.31%, 15.27% and 17.59% when pitch raised from 2 to 10 for S1,S2, S3 respectively. The results align with the research conducted by NIE *et al.* [31]. They investigated the impact of increasing the pitch from 150 mm to 300 mm and from 150 mm to 450 mm on a double-box column section composed of four channels. This alteration reduced the load-carrying capacity of the built-up columns by 1.8% and 3.4%, respectively.

In order to obtain an optimum pitch for the section, a parametric study has been conducted for various pitch values using FEM for CFS BU-C0.8. Stimulated results of parametric study done for specimen S1BU-C0.8P5, S1BU-C0.8P2, S2BU-C0.8P5 and S2BU-C0.8P are shown in Figure 13. The axial load capacity of CFS BU-C column for various pitches was represented in Figure 14 for sections S1, S2, and S3. The optimum value of pitch obtain is shown in Table 3.

From the result it has been observed that the percentage of increase in axial load is maximum for pitch 4 in case of S1 and S2 which is 8.23% and 9.2% higher when compared with pitch 2. For S3, the optimum increase in axial load is obtained for a pitch 6 in which an increase of 10.25% is achieved compared to pitch 2. The experimental result of specimen S3BU-C0.8P6 confirms well with the FEM results. It is noted that the higher the cross section particularly the depth along with a greater number of spot weld yields higher axial load for CFS BU-C.

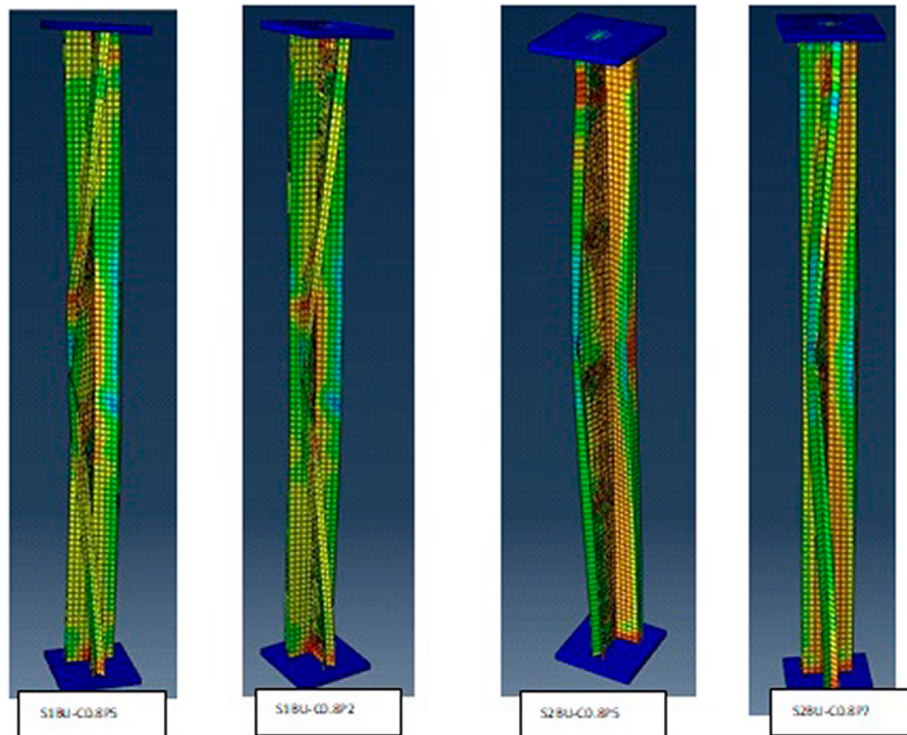


Figure 13: Stimulated model of parametric studies.

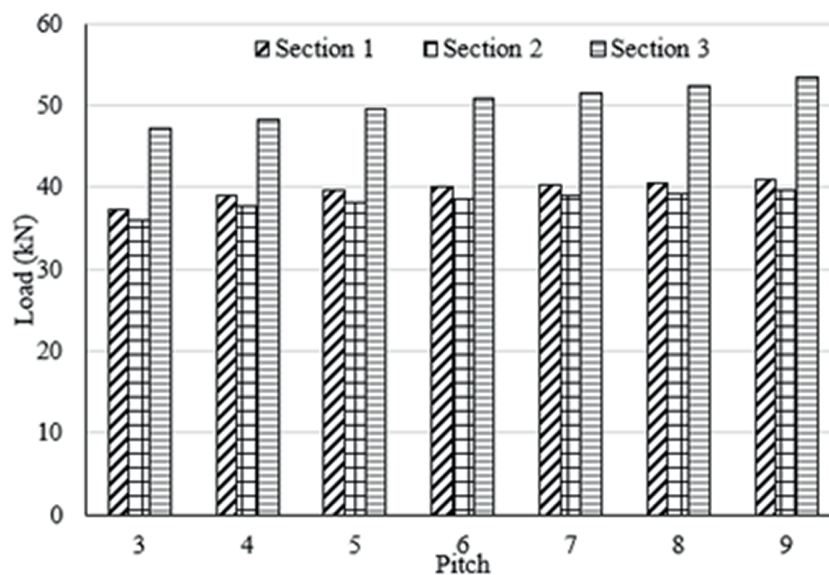
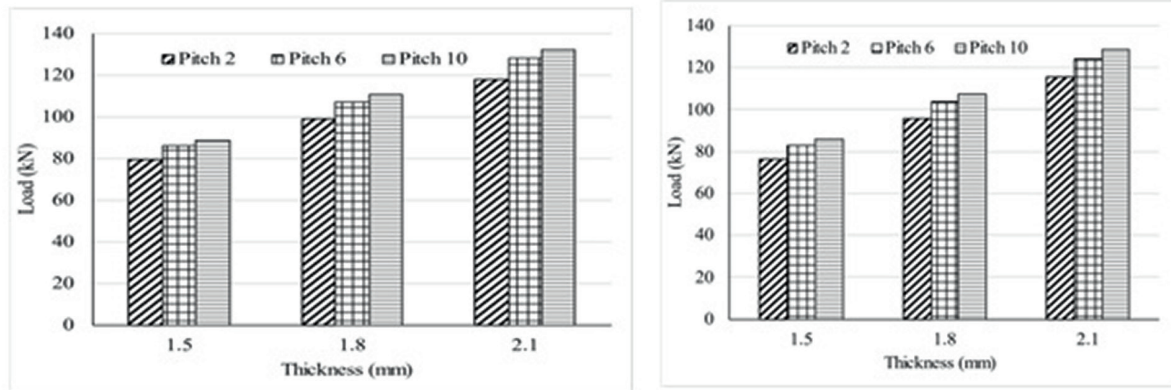


Figure 14: Variation of load and pitch for S1, S2, S3 for 0.8 thickness.

**Table 3:** Details of parametric studies for optimum pitch.

| S NO | SECTION  | THICKNESS IN mm | NO OF PITCH | PITCH OF SPOT WELDING IN mm | NC, FEA (kN) | FAILURE MODE |
|------|----------|-----------------|-------------|-----------------------------|--------------|--------------|
| 1.   | 75 × 50  | 0.8             | 4           | 225                         | 38.98        | FT           |
| 2.   | 80 × 40  | 0.8             | 4           | 225                         | 37.64        | FT           |
| 3.   | 100 × 75 | 0.8             | 6           | 150                         | 50.95        | FT           |



**Figure 15:** Variation of load and thickness for Pitch 2, 6, 10 for S1, S2.

**Table 4:** Details of parametric studies on Length of column.

| S.NO | SECTION | LENGTH IN mm | NO OF PITCH | PITCH OF SPOT WELDING IN mm | NC, FEA (kN) | FAILURE MODE |
|------|---------|--------------|-------------|-----------------------------|--------------|--------------|
| 1    | 75 × 50 | 1200         | 2           | 450                         | 32.70        | FT           |
| 2    | 75 × 50 | 1200         | 6           | 150                         | 37.13        | FT           |
| 3    | 75 × 50 | 1200         | 10          | 90                          | 38.25        | FT           |

**6.2. Effect of thickness**

FEM were stimulated on specimen S1 and S2 for higher value of thickness of 1.5 mm, 1.8 mm and 2.1 mm for pitch 2, 6 and 10. The results were displayed in the Figure 15. It is noted that there is an increase in axial compressive load values by 24.11% and 25.06% for S1 and S2 respectively when thickness increased from 1.2 mm to 1.5 mm.

It is observed from both experiment and FEM , the higher the thickness of specimen results in higher axial load taking capacity provided the number of spot weld connections along with its pitch get increased thereby confirming the composite behaviour of the column. Both Experimental and Analytical findings are in alignment with the conclusions of ANANTHI *et al.* [8].

**6.3. Effect of length**

The parametric study on varying slenderness ratio were made by increasing the length of column to 1.2 m for the specimen S1 for three different pitch values of 2, 6 and 10 for a thickness of 0.8 mm. The axial compressive load for these specimens for varying pitch were displayed in Table 4. From the result it is observed that an decrease in axial capacity of 9.23%,7.21% and 7.11% were noted when length of column increases from 1 m to 1.2 m for pitch 2, 6 and 10.

Length of specimen along with pitch plays an important factor in determining axial load capacity of BU-C for calculating flexural and torsional buckling stress. Interrelation between length and pitch of weld spacing has to be included in determining the flexural and flexural torsional stress of built-up columns which will vary the axial capacity of BU-C column for slender columns [32].

## 7. SUMMARY AND CONCLUSION

The specimen tested is unique in three aspects namely, two individual specimens are joined by spot welding, it is singly symmetrical about the vertical axis and out of four lips provided, two lips are inclined at an angle of 135°. Experimental test were conducted on 27 specimens for three different sections for varying thickness and pitch. From the buckling mode and axial load capacity of built up column, it is inferred that pitch of spot welding is more pronounced for higher thickness and higher B/D ratio specimen to include the effect built up action of the specimen.

The Finite element modeling was simulated using Abacus to validate the experimental results. Both experimental testing and FE modeling have revealed that CFS BU-C can experience failure in either flexural or torsional flexural buckling. Using the validated FE models, parametric study was conducted for various pitch, thickness and length of the sections. Axial load capacity of the column and its buckling behaviour depends on the pitch of spot welding, thickness and length of specimen.

- Effect of pitch of spot welding-It is observed that an increase in pitch, combined with an increase in the number of spot welds in a row, results in a higher axial load-carrying capacity of the CFS BU-C.
- Effect of thickness-It is noted that the increase in thickness should be supplemented with increase in pitch to get composite behavior thereby increasing its load carrying capacity
- Effect of length-It is inferred that the increase in length should be augmented with increase in pitch and number of spot welding in a row to increase the load carrying capacity of specimen.

Considering the effect of pitch in back to back built up section in calculating global slenderness ratio alone is not sufficient and it is recommended to consider the above three factors and their inter relation with one another as critical parameter in determining the global buckling stress in codal provisions. The outcomes of experimental tests and analytical modeling for 27 Cold-Formed Steel Built-Up Channels (CFS BU-C) are presented. Validated Finite Element (FE) models were employed for parametric studies involving varied values of pitch, thickness, and length. The axial compressive strength, along with the corresponding failure modes, is tabulated, providing interpretation for enhanced understanding.

## 8. BIBLIOGRAPHY

- [1] YOUNG, B., JU, C., “Design of cold-formed steel built-up closed sections with intermediate stiffeners”, *Journal of Structural Engineering*, v. 134, n. 5, pp. 727–737, 2008. doi: [http://dx.doi.org/10.1061/\(ASCE\)0733-9445\(2008\)134:5\(727\)](http://dx.doi.org/10.1061/(ASCE)0733-9445(2008)134:5(727)).
- [2] VY, S.T., MAHENDRAN, M., SIVAPRAKASAM, T. “Built-up nested cold-formed steel compression members subject to local or distortional buckling”, *Journal of Constructional Steel Research*, v. 182, pp. 106667, 2021. doi: <https://doi.org/10.1016/j.jcsr.2021.106667>.
- [3] ELLOBODY, E., YOUNG, B., “Structural performance of cold-formed high strength stainless steel columns”, *Journal of Constructional Steel Research*, v. 61, n. 12, pp. 1631–1649, 2005. doi: <http://dx.doi.org/10.1016/j.jcsr.2005.05.001>.
- [4] ANBARASU, M., BHARATH KUMAR, P., SUKUMAR, S., “Study on the capacity of cold-formed steel built-up battened columns under axial compression”, pp. 2271–2283, 2014. doi: <https://doi.org/10.1590/S1679-78252014001200009>.
- [5] ANANTHI, G.B.G., ROY, K., GHOSH, B., *et al.*, “An investigation on stiffened cold-formed steel unequal angle box section columns”, *Journal of Building Engineering*, v. 76, Oct. 2023, pp. 106989. doi: <https://doi.org/10.1016/j.jobbe.2023.106989>.
- [6] ANANTHI, G.B.G., ROY, K., LIM, J.B.P., “Behavior and strength of back-to-back built-up cold-formed steel unequal angle sections with intermediate stiffeners under axial compression”, *Steel and Composite Structures*, v. 42, n. 1, pp. 1–22, 2022. doi: <https://doi.org/10.12989/scs.2022.42.1.001>.
- [7] GURUPATHAM, B.G.A., ROY, K., RAFTERY, G.M., *et al.*, “Influence of intermediate stiffeners on axial capacity of thin-walled built-up open and closed channel section columns”, *Buildings*, v. 12, n. 8, pp. 1071, 2022. doi: <https://doi.org/10.3390/buildings12081071>.
- [8] ANANTHI, G.B.G., PALANI, G.S., IYER, N.R., “Numerical and theoretical studies on cold-formed steel unlipped channels subjected to axial compression”, *Latin American Journal of Solids and Structures*, v. 12, n. 1, pp. 1–17, Jan. 2015. doi: <https://doi.org/10.1590/1679-78251178>.
- [9] LOUGHLAN, J., YIDRIS, N., JONES, K., “The failure of thin-walled lipped channel compression members due to coupled local-distortional interactions and material yielding”, *Thin-walled Structures*, v. 61, pp. 14–21, 2012. doi: <http://dx.doi.org/10.1016/j.tws.2012.03.025>.

- [10] CRAVEIRO, H.D., RODRIGUES, J.P.C., LAÍM, L., “Buckling resistance of axially loaded cold-formed steel columns”, *Thin-Walled Structures*, v. 106, pp. 358–375, Sep. 2016. doi: <https://doi.org/10.1016/j.tws.2016.05.010>.
- [11] KANTHASAMY, E., HUSSAIN, J., THIRUNAVUKKARASU, K., *et al.*, “Flexural behaviour of built-up beams made of optimised sections”, *Buildings*, v. 12, n. 11, pp. 1868, 2022. doi: <http://dx.doi.org/10.3390/buildings12111868>.
- [12] DAI, Y., ROY, K., FANG, Z., *et al.*, “A critical review of cold-formed built-up members: developments, challenges, and future directions”, *Journal of Building Engineering*, v. 76, pp. 107255, 2023. doi: <https://doi.org/10.1016/j.jobe.2023.107255>.
- [13] TAO, F., COLE, R., MOEN, C.D., “Monotonic and cyclic backbone response of single shear cold-formed steel screw-fastened connections”, *The International Colloquium on Stability and Ductility of Steel Structures*, pp. 629–645, 2016.
- [14] ABU-HAMD, M., “Experimental study on screw connections in cold-formed steel walls with cement sheathing”, *Advances in Structural Engineering*, v. 22, n. 9, pp. 2033–2047, 2019. doi: <https://doi.org/10.1177/1369433219829808>.
- [15] TING, T.C.H., ROY, K., LAU, H.H., *et al.*, “Effect of screw spacing on behaviour of axially loaded back-to-back cold-formed steel built-up channel sections”, *Advances in Structural Engineering*, v. 21, n. 3, pp. 474–487, 2017. doi: <https://doi.org/10.1177/1369433217719986>.
- [16] PATIL, D.V., SANKPAL, G.A., “A review on effect of spot weld parameters on spot weld strength”, *International Journal of Engineering Development and Research*, v. 3, n. 1, pp. 1–6, 2014.
- [17] CHANDRAMOHAN, D.L., ROY, K., TAHERI, H., *et al.*, “A state of the art review of fillet welded joints”, *Materials (Basel)*, v. 15, n. 24, pp. 8743, 2022. doi: <http://dx.doi.org/10.3390/ma15248743>. PubMed PMID: 36556549.
- [18] YUAN, H.X., WANG, Y.Q., GARDNER, L., *et al.*, “Local–overall interactive buckling of welded stainless steel box section compression members”, *Engineering Structures*, v. 67, pp. 62–76, 2014. doi: <http://dx.doi.org/10.1016/j.engstruct.2014.02.012>.
- [19] EUROPEAN COMMITTEE FOR STANDARDIZATION, *EN 1993-1-3 Eurocode 3, Design of Steel Structures – Part 1-3: General Rules. Supplementary Rules for Cold-Formed Thin Gauge Members and Sheeting*, Brussels, Cen, 2006.
- [20] AMERICAN IRON AND STEEL INSTITUTE. *AISI S100, North American Specification for the Design of Cold-Formed Steel Structural Members*, Washington, AISI, 2016.
- [21] BAN, H., SHI, G., SHI, Y., *et al.*, “Overall buckling behavior of 460 MPa high strength steel columns: experimental investigation and design method”, *Journal of Constructional Steel Research*, v. 74, pp. 140–150, 2012. doi: <http://dx.doi.org/10.1016/j.jcsr.2012.02.013>.
- [22] HE, Z., ZHOU, X., “Strength design curves and an effective width formula for cold-formed steel columns with distortional buckling”, *Thin-walled Structures*, v. 79, pp. 62–70, 2014. doi: <http://dx.doi.org/10.1016/j.tws.2014.02.004>.
- [23] MARTINS, A.D., CAMOTIM, D., DINIS, P.B., “The direct strength design of cold-formed steel columns failing in local distortional interactive modes”, *Thin-Walled Structures*, v. 120, pp. 432–445. doi: <https://doi.org/10.1016/j.tws.2017.06.027>.
- [24] MAIA, W.F., VIEIRA JUNIOR, L.C.M., SCHAFFER, B.W., *et al.*, “Experimental and numerical investigation of cold-formed steel double angle members under compression”, *Journal of Constructional Steel Research*, v. 121, pp. 398–412, 2016. doi: <https://doi.org/10.1016/j.jcsr.2016.03.003>.
- [25] ZHOU, X., CHEN, M., “Experimental investigation and finite element analysis of web-stiffened cold formed lipped channel columns with batten sheets”, *Thin-walled Structures*, v. 125, pp. 38–50, 2018. doi: <http://dx.doi.org/10.1016/j.tws.2018.01.006>.
- [26] DAI, Y., FANG, Z., ROY, K., *et al.*, “Optimal design of cold-formed steel face-to-face built-up columns through deep belief network and genetic algorithm”, *Structures*, v. 56, pp. 104906, Oct. 2023. doi: <http://dx.doi.org/10.1016/j.istruc.2023.104906>.
- [27] AMERICAN SOCIETY FOR TESTING AND MATERIALS, *E8/E8M-13a Standard Test Methods for Tension Testing of Metallic Materials*, West Conshohocken, ASTM, 2013.
- [28] HUANG, Y., YOUNG, B., “The art of coupon tests”, *Journal of Constructional Steel Research*, v. 96, pp. 159–175, 2014. doi: <http://dx.doi.org/10.1016/j.jcsr.2014.01.010>.

- [29] UNGUREANU, V., BOTH, I., BURCA, M., *et al.*, “Experimental and numerical investigations on built-up cold-formed steel beams using resistance spot welding”, *Thin-walled Structures*, v. 161, pp. 107456, 2021. doi: <http://dx.doi.org/10.1016/j.tws.2021.107456>.
- [30] YOUNG, B., CHEN, J., “Design of cold-formed steel built-up closed sections with intermediate stiffeners”, *Journal of Structural Engineering*, v. 134, n. 5, pp. 727–737, 2008. doi: [http://dx.doi.org/10.1061/\(ASCE\)0733-9445\(2008\)134:5\(727\)](http://dx.doi.org/10.1061/(ASCE)0733-9445(2008)134:5(727)).
- [31] NIE, S., ZHOU, T., EATHERTON, M.R., “Compressive behavior of built-up double-box columns consisting of four cold-formed steel channels”, *Engineering Structures*, v. 222, pp. 111133, 2020. doi: <https://doi.org/10.1016/j.engstruct.2020.111133>
- [32] VY, S.T., MAHENDRAN, M., “Behaviour and design of slender built-up nested cold formed steel compression members”, *Engineering Structures*, v. 241, pp. 112446, 2021. doi: <https://doi.org/10.1016/j.engstruct.2021.112446>.